SPATIO-TEMPORAL VARIABILITY OF PRECIPITATION IN SOUTHEAST ASIA ANALYZED USING THE EMPIRICAL ORTHOGONAL FUNCTION (EOF) TECHNIQUE

Soo Chin Liew, Aik Song Chia and Leong Keong Kwoh

Centre for Remote Imaging, Sensing and Processing (CRISP), National University of Singapore
Blk SOC-1 Level 2 Lower Kent Ridge Road, Singapore 119260

1. INTRODUCTION

Recently global climate change has been a great environmental concern in many countries. Most of the populations in the Southeast Asia region reside in coastal zones, which will be affected by sea level rise due to climate change. Change in precipitation, land and sea surface temperature and cloud cover will have effects on agriculture, forest vegetation, ecology and living habitats. In this paper, we focus our study on the spatio-temporal variability of rainfall in the Southeast Asia region. The data set used is the TRMM 3B43v6 monthly precipitation product which was calibrated with monthly rain gauge data from the Global Precipitation Climatology Project (GPCP) [1]. The empirical orthogonal function (EOF) analysis [2, 3] is used to investigate the spatial and temporal variations of precipitation rate. Basically, the EOF analysis decomposes the rainfall data into several modes of variations. Each mode can be associated with one or several mechanisms of variations. We found that the strongest mode is associated with the annual variations mainly due to the seasonal monsoons. The second and third modes are moderately correlated with El-Nino. Possible associations with global warming are being investigated.

2. TRMM 3B43 PRECIPITATION DATASET

The Tropical Rainfall Measuring Mission (TRMM) satellite carries an active Precipitation Radar (PR) instrument besides the passive Thematic Microwave Imager (TMI). The TRMM Multisatellites Precipitation Analysis (TMPA) products are generated using data from all the available sensors. TMPA products are quasi-global, multiyear combined sensor precipitation estimates of rain rate [1]. The TRMM 3B43v6 monthly average rainrate product on a 0.25^{o} spatial grid is used for our analysis. This is a combined multi-sensor product calibrated with monthly rain gauge analysis from the Global Precipitation Climatology Project (GPCP) [1]. The 3B43 dataset has been validated by several research groups [5, 6]. The TRMM 3B43v6 global precipitation rate dataset was obtained from Goddard Earth Science Data and Information Services Center (GES DISC). The global precipitation data consist of the mean monthly rain rate, in mm per hour, resampled on 0.25 degree grids, covering the period from Jan 1998. We extract a subset over the Southeast Asia region (80^{o}E to 130^{o}E, 15^{o}S to

25°N) for analysis. To determine correlations with El-Nino, we use the Ocean Nino Index (ONI) produced by NOAA's Climate Prediction Center. The ONI is defined as the 3 month running mean of ERSST.v3b SST anomalies in the Niño 3.4 region (i.e. 5°N-5°S, 120°-170°W). The onset of an El Niño episode is declared when the ONI exceeds 0.5°C.

3. METHODS

The EOF analysis is similar to the principal components analysis (PCA) commonly used for decorrelating a set of variables. The dataset of the observed parameter can be treated as a function $s(x, y, t)$ of the spatial coordinates (x, y) and time t. The EOF analysis basically decomposes $s(x, y, t)$ into a series of orthogonal functions $f_i(x, y)$ of the spatial coordinates only. The temporal variation is captured in a series of temporal functions $g(t)$ such that,

$$s(x, y, t) = \sum_{i=1}^{N} f_i(x, y) g_i(t) \qquad (1)$$

where N is the total number of observations made in time. The EOF's $f_i(x, y)$ and their respective coefficients $g(t)$ can be found by solving the eigenvalue equation constructed from the covariance matrix of $s(x, y, t)$. The orthogonal functions $f_i(x, y)$ are arranged in decreasing order of the corresponding eigenvalues of the covariance matrix. Thus, the first few orthogonal functions usually account for most of the spatial variance that exists in the dataset.

4. RESULTS

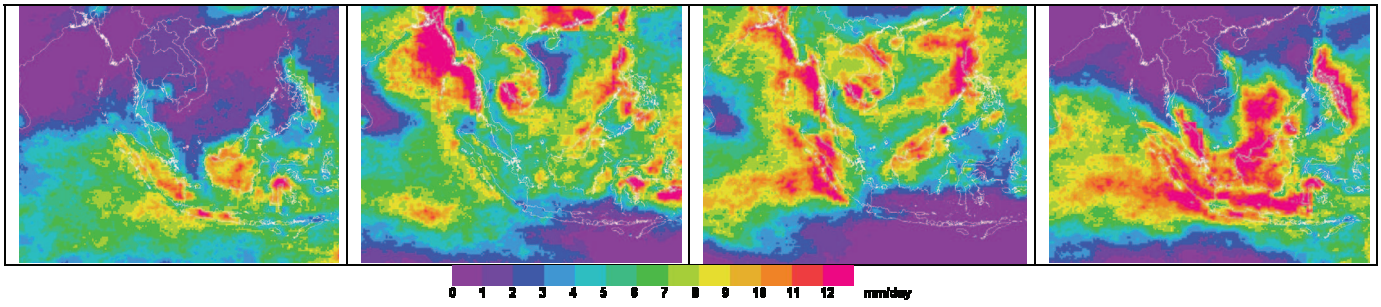

Fig. 1: Average monthly rainrate for the months of (left to right) March, June, September and December.

The average monthly rainrate for the months of March, June, September and December are shown in Figure 1. The continental part is dry in northern winter and spring while the insular part is generally wet. The northern region becomes wetter in summer and fall.

EOF analysis is performed on the precipitation rate data set. The first three modes are shown in Fig. 2. Mode 1 corresponds to the seasonal variation of precipitation as illustrated by the sinusoidal variations of the temporal coefficients (bottom left of Fig. 2). This oscillation has a maximum in June-July and minimum in Dec-Jan. The spatial variation of this mode is illustrated in the corresponding EOF1 (top left of Fig. 2). Positive values of EOF1 indicate the temporal variation in phase with the variations of the temporal coefficients while negative

values indicate an out of phase variation. These observations are in generally agreement with the monthly mean precipitation rate shown in Fig. 1.

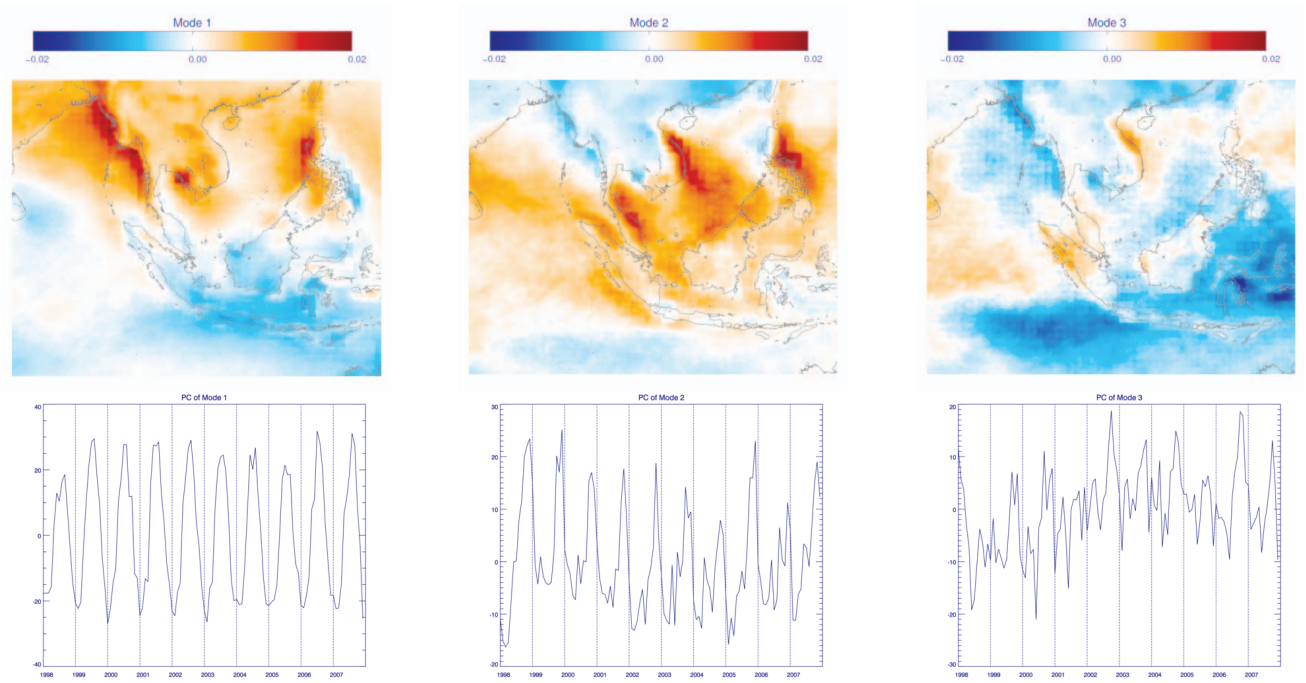

Fig. 2: The first three EOF modes, (top row, left to right) EOF1, EOF2 and EOF3. The corresponding temporal coefficients are shown on the bottom row.

The second mode EOF2 shows a more erratic temporal pattern. Fourier analysis of the temporal coefficients shows two dominant periodic components of 12 and 6 months cycles. The EOF2 temporal coefficients are shown in Fig. 3, together with the climatological trend line composed from the average monthly values superimposed on a linear trend. In this case, the linear trend has a slight but non significant negative slope. The deviation of the EOF2 temporal coefficients from the climatological trend line (EOF2 temporal anomaly) is shown in Fig. 4. It is interesting to note that the EOF2 temporal anomaly seems to vary in anti-phase with the Ocean Nino Index, though higher frequency oscillations are also present. Indeed, regression of the EOF2 anomaly with the Ocean Nino Index (Fig. 5 left) gives a coefficient of determination $R^2 = 0.47$, i.e. about 47% of the variance in EOF2 anomaly can be attributed to El-Nino. A similar analysis is performed on EOF3 and the EOF3 temporal anomaly exhibits a positive correlation with Nino Index (Fig. 5 right) with $R^2 = 0.38$.

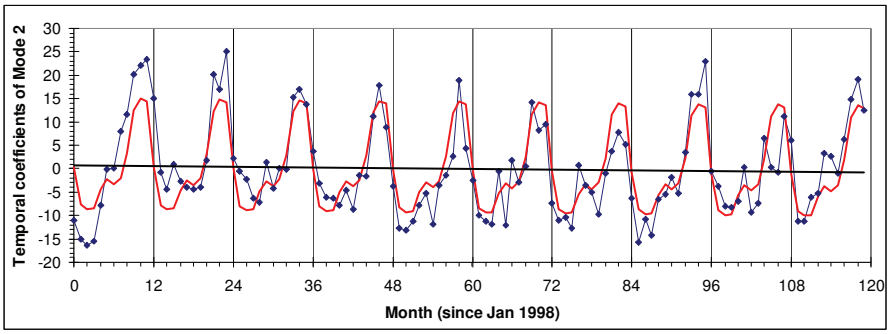

Fig. 3: Temporal coefficients of EOF2. The red line is the climatological trend line composed from the average monthly values superimposed on a linear trend.

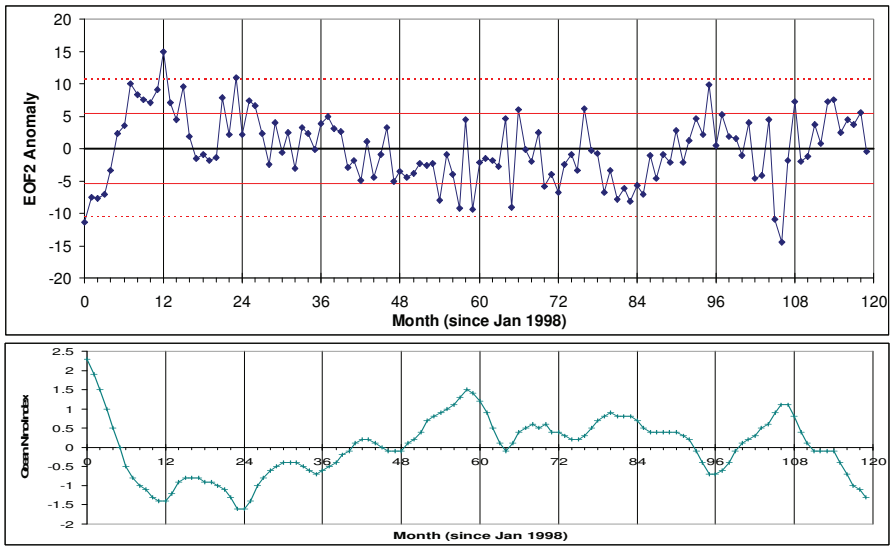

Fig. 4: EOF2 temporal anomaly (top) and the Ocean Nino Index (bottom) from Jan 1998 to Dec 2007.

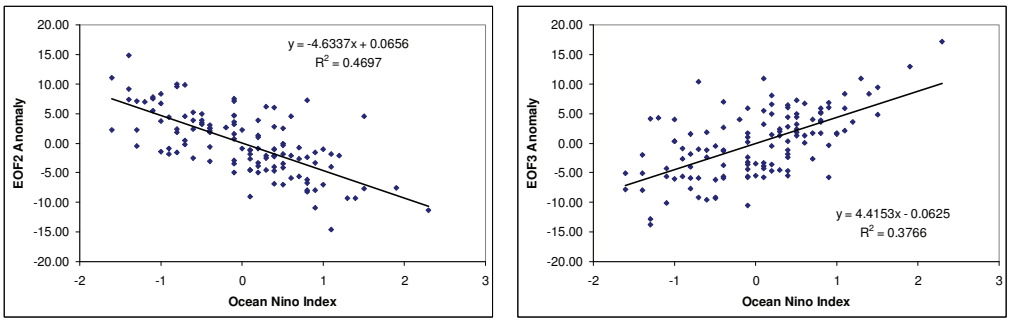

Fig. 5: Linear regressions of EOF2 (left) and EOF3 (right) temporal anomalies with Ocean Nino Index

5. CONCLUSIONS

EOF analysis is a useful tool in analyzing climate data. Our results show that EOF analysis can decompose the spatial and temporal variations of precipitation rate into several modes. The strongest mode is associated with the seasonal monsoons while the second and third modes are partly associated with El-Nino. In the full paper, we will explore the possible associations with global warming by correlating with the global warming index composed from land or sea surface temperature. The higher order modes will also be investigated to establish relations with other climate forcing factors.

6. REFERENCES

[1] Huffman, G. et al., "The TRMM multisatellite precipitation analysis (TMPA): Quasi-global, multiyear, combined-sensor precipitation estimates at fine scales," *Journal of Hydrometeorology*, vol. 8, pp. 38-55, Feb 2007.

[2] Lorenz, E. N., "Empirical orthogonal functions and statistical weather prediction," Sci. Rep. No. 1, Statistical Forecasting Project, MIT, Cambridge, MA, 48pp., 1956.

[3] Bjornsseon, H. and S. A. Venegas, " A manual for EOF and SVD analyses of climate data," McGill University CCGCR Report No. 97-1, Montréal, Québec, 52pp., 1997.

[4] Levizzani, V., R. Amorati, F. Meneguzzo, "A Review of Satellite-based Rainfall Estimation Methods", European Commission Project MUSIC Report (EVK1-CT-2000-00058), 2002.

[5] Dinku, T. et al., "Validation of satellite rainfall products over East Africa's complex topography," International Journal of Remote Sensing, vol. 28, pp. 1503-1526, Apr 2007.

[6] Islam, M. and H. Uyeda, "Use of TRMM in determining the climatic characteristics of rainfall over Bangladesh," Remote Sensing of Environment, vol. 108, pp. 264-276, Jun. 2007.